

# Ionization of atomic hydrogen by antiproton impact: A direct solution of the time-dependent Schrödinger equation

Xiao-Min Tong,<sup>1,\*</sup> Tsutomu Watanabe,<sup>1,2</sup> Daiji Kato,<sup>1</sup> and Shunsuke Ohtani<sup>1,2</sup>

<sup>1</sup>“Cold Trapped Ions” Project, ICORP, Japan Science & Technology Corporation (JST), Axis Chofu Building 3F, 1-40-2 Fuda Chofu, Tokyo 182-0024, Japan

<sup>2</sup>University of Electro-Communications, Chofu, Tokyo 182-0021, Japan

(Received 12 February 2001; published 11 July 2001)

We present a theoretical study on the ionization of a H atom by antiproton impact in a wide energy range (from 0.1 to 1000 keV). Taking a semiclassical approximation, in which the relative motion of the antiproton with respect to the atomic nucleus is described by classical mechanics, the time evolution of the electron motion is described by quantum mechanics. The time evolution of the electronic wave function is propagated by the split-operator method with a generalized pseudospectral method in the energy representation. Particular attention is paid to the numerical accuracy and numerical convergence. The maximum numerical uncertainty is estimated to be less than 3% at the lower-energy side by comparison of the ionization cross sections calculated with three schemes. The trajectory effect is also studied by comparison with the ionization cross sections calculated with a straight-line trajectory and a curved trajectory. The calculated ionization cross sections of H atoms by antiproton impact are compared with other calculations. Our calculated results are in good agreement with the experimental measurement.

DOI: 10.1103/PhysRevA.64.022711

PACS number(s): 34.50.Fa, 34.10.+x, 36.10.-k

## I. INTRODUCTION

The ionization of a hydrogen atom by antiproton ( $\bar{p}$ ) impact is one of the simplest and most fundamental processes in atom-ion collision physics. Different from H + proton collisions, the charge-transfer channel is totally eliminated in H +  $\bar{p}$  collisions, which makes the theoretical investigation easier. There are many theoretical works [1–15] on this simple subject. In the high-energy region, most of the calculations agree with the experimental results [16]. The discrepancies among the theoretical calculations appear in the medium- to lower-energy region ( $E < 100$  keV). The existing experimental data [16] are smaller than most of the calculations in the energy region from 30 to 100 keV. Meanwhile, the experimental error bar is so large in this energy region that the experimental data cannot be used to judge which calculation is more reliable. Furthermore, experimental research using slow antiprotons was prepared under the project of ASACUSA [17] at the Antiproton Decelerator in CERN. This group will measure the atomic collision process using keV antiproton beams. The experimental data for the ionization process of a H atom by low-energy  $\bar{p}$  impact will be available in the near future. Apart from the experimental development, the trajectory effect in the lower collision energy region is not well studied in the impact-parameter method. All these factors call for a further theoretical study.

The ionization of a H atom by antiproton impact in the high-energy region can be studied by the Born approximation [1], which only depends on the target stationary wave function. In the intermediate-energy region, the Born approximation should be modified by using the distorted-wave (DW) method [5], which includes the deformation of the

target stationary wave function by the projectile. Both methods cannot be used to study the ionization process in H +  $\bar{p}$  collisions over a wide energy range. Especially in the lower-energy region, the Born and DW methods are no longer valid. The ionization of H atoms by an antiproton was calculated by the classical trajectory Monte Carlo (CTMC) method [3,4,7]. The CTMC method treats the problem in the same way as the experimental measurement does within the limit of purely classical mechanics. The CTMC method gave plausibly good results in spite of its weak point. The validity of the CTMC method for the atomic scattering problem has never been proven since the H atom is a quantum system. There are also several semiclassical methods to study the ionization of H atom by antiproton impact. In the semiclassical method, the electronic motion is described by quantum mechanics, and the relative motion between the proton and antiproton is described by classical mechanics. Such a method can also be called an impact parameter method. Recently, there were many close-coupling (CC) calculations [6,8,11–13] based on the impact parameter method. With advances in computational technology, recently there were several studies [7,10,14,15] that directly solved the time-dependent Schrödinger equation (TDSE) for the electronic motion. In TDSE calculations, although the physical picture is very intuitive, the numerical accuracy and numerical convergence are a large challenge, especially in the lower-energy region (below 1 keV).

In our previous papers [18,19], we studied the excitation and charge-transfer processes of proton impact on H atoms and He<sup>+</sup> ions by directly solving the time-dependent Schrödinger equation with the split-operator method and a generalized pseudospectral method in the energy representation based on the impact-parameter method. Our results are in good agreement with experiments. Since our method can describe the charge-transfer and impact excitation well, we will

\*Email address: tong@hci.jst.go.jp

study the ionization process in the  $H + \bar{p}$  collisions in a wide energy region (from 0.1 to 1000 keV) by this method. Since the formation of protoniums becomes significant [3,20,21] only at a collision energy lower than the ionization energy (13.6 eV) of H atoms, we will not consider the formation of protoniums in the energy region we study in the present paper. In the calculations, the highly excited states ( $n > 10$ ) are not well described. The numerical uncertainty due to the highly excited states is estimated to be less than 3% on the lower-energy side. The estimation is based on the ionization cross sections calculated with three schemes, which can give the upper limit and roughly the lower limit of the ionization cross sections. Note that we cannot directly study the formation of protoniums with our present method. The formation for the protoniums should be studied in a fully quantum-mechanical way. In the following, we will give a brief introduction of our theoretical method in Sec. II, present the details about the calculation and convergence check in Sec. III, and present our results and discussion in Sec. IV.

## II. THEORETICAL METHOD

The ionization of a H atom by antiproton impact can be studied by solving the following time-dependent Schrödinger equation with a classic trajectory for the nucleus motion, (atomic units with  $\hbar = m = e = 1$  are used throughout unless explicitly stated otherwise),

$$i \frac{\partial}{\partial t} \psi(\mathbf{r}, t) = H(t) \psi(\mathbf{r}, t), \quad (1)$$

with

$$H = -\frac{\nabla^2}{2} - \frac{1}{r} + \frac{1}{|\mathbf{R} - \mathbf{r}|}, \quad (2)$$

$$\mu \ddot{\mathbf{R}} = -\nabla V(\mathbf{R}), \quad (3)$$

$$V(\mathbf{R}) = -\frac{1}{R} + \int \frac{\psi^*(\mathbf{r}, t) \psi(\mathbf{r}, t)}{|\mathbf{R} - \mathbf{r}|} d\mathbf{r}. \quad (4)$$

Here we assume that  $\bar{p}$  approaches the target H atom, which rests at the origin, along the  $z$  direction with a velocity  $v$ , and the impact parameter  $b$  is along the  $x$  direction. We also assume that the relative motion of the incident  $\bar{p}$  with respect to the target hydrogen atom follows a classical trajectory from Eq. (3) (CT) or a simple straight line trajectory [ $\mathbf{R} = (b, 0, z_0 + vt)$ ] (ST). Equation (1) can be solved by the second-order split-operator method, with a generalized pseudospectral grid in the energy representation [18,19,22], as

$$\psi(t + \Delta t) = e^{-iH_0 \Delta t/2} e^{-i\tilde{V}(t) \Delta t} e^{-iH_0 \Delta t/2} \psi(t), \quad (5)$$

where

$$\psi(t) = \sum_{l,m} \sum_k C_{lm}^k(t) \phi_l^k(r) Y_{lm}(\hat{\Omega}), \quad (6)$$

$$H_0 = -\frac{\nabla^2}{2} - \frac{1}{r}, \quad (7)$$

$$\tilde{V}(t) = \frac{1}{|\mathbf{R} - \mathbf{r}|}. \quad (8)$$

To propagate the wave function in Eq. (5), we use spherical coordinates, and the radial part is discretized by the generalized pseudospectral grid method [23]. The first step is to map the semi-infinite domain  $[0, \infty)$  or  $[0, r_{max}]$  into the finite domain  $[-1, 1]$  using a nonlinear mapping  $r = r(x)$ , followed by the Legendre pseudospectral discretization. A suitable algebraic mapping for atomic structure calculations is provided by the form

$$r = r(x) = L \frac{1+x}{1-x+\alpha}, \quad (9)$$

where  $L$  and  $\alpha = 2 \times L/r_{max}$  are mapping parameters. The introduction of nonlinear mapping usually leads to either an asymmetric or a generalized eigenvalue problem. Such undesirable features may be removed by the use of a symmetrization procedure [23]. Thus, by defining

$$\phi_l(r) = \sqrt{r'(x)} \chi_l(r(x)), \quad (10)$$

one finds the transformed Hamiltonian possesses the following symmetrized form:

$$\hat{H}_l^o(x) = -\frac{1}{2} \frac{1}{r'(x)} \frac{d^2}{dx^2} \frac{1}{r'(x)} + V_l(r(x)), \quad (11)$$

where  $V_l = [l(l+1)/2r^2] - (1/r)$ , leading Eq. (11) to a symmetric eigenvalue problem. In the Legendre pseudospectral method, the collocation points  $\{x_j\}$  are the roots of the polynomials  $P'_{N+1}(x)$ , where  $N$  is the total number of grid points used in the discretization. In such a discretized scheme, the Hamiltonian  $\hat{H}_l^o(x)$  [Eq. (11)], can be represented by the matrix form

$$[H_l^o]_{ij} = (D_2)_{ij} + V_l(x_i) \delta_{ij}, \quad (12)$$

with

$$(D_2)_{ij} = \frac{1}{r'(x)} \frac{(N+1)(N+2)}{6(1-x_i^2)} \frac{1}{r'(x)}, \quad i=j. \quad (13)$$

$$(D_2)_{ij} = \frac{1}{r'(x)} \frac{1}{(x_i - x_j)^2} \frac{1}{r'(x)}, \quad i \neq j. \quad (14)$$

The eigenvalues and eigenfunctions of  $\hat{H}_l^o$  will be denoted by  $\{\epsilon_k(l)\}$  and  $\{\chi_{ki}(l)\}$ , respectively. The propagation of the wave function can be performed in Eq. (5).

The advantages of the numerical method are that (1) we use a nonequal space grid with a denser grid in the physical important region (interaction region), and a wider grid in the outer region to save the computer time; and (2) we propagate the time-dependent wave function in an energy representa-

tion which is more effective and accurate than that in the kinetic representation [24,25]. A detailed numerical procedure can be found in Refs. [18,19,22]. With this impact parameter method, we can propagate the wave function from  $t=0 \rightarrow T$ , with an impact parameter  $b$  along the  $x$  direction and a projectile velocity  $v$  along the  $z$  direction, starting from  $z_0$ . The initial wave function is located in the target ground state. When the projectile passes through the target or is far from the target, we can obtain the excitation or ionization probabilities as

$$P(T,b) = |\langle \psi(T) | \psi_f \rangle|^2, \quad (15)$$

where  $\psi_f$  is the time-independent (excited or continuum states) wave function centered at the target H atom. The corresponding cross sections can be obtained as

$$\sigma = 2\pi \int P(T,b) b db. \quad (16)$$

Our grid structure is centered at the target atom and, in some sense, it forms a ‘‘complete’’ basis set for the target atom, which is similar to one center close-coupling orbitals [12,13]. Different from the close-coupling method, we do not need to evaluate the interaction matrix, which can save a considerable computer time.

### III. NUMERICAL CALCULATION AND CONVERGENCE CHECK

Based on the split-operator method with the time-dependent generalized pseudospectral in the energy representation [18,19,22], we solved the time-dependent Schrödinger equation to study H +  $\bar{p}$  collisions. The impact ionization cross sections were calculated in a wide energy range (from 0.1 to 1000 keV). All the calculations were performed in a 4 PC Linux cluster with a Pentium III 400 MHz CPU. The parameters used in the calculations are  $r_{max} = 200$  a.u., 15 partial waves, and 2000–6000 time steps. The radial part is discretized into 150 *nonuniform* pseudospectral grid points. At  $t=0$ , the projectile  $\bar{p}$  starts from  $z_0 = -20$  a.u. with the impact parameter  $b$  along the  $x$  direction. The initial electronic wave function is located at the target H  $1s$  state in the origin of the coordinates. The time-dependent wave function is propagated by Eq. (1) with a projectile trajectory from Eq. (3), or a straight-line trajectory from  $z_0$  to  $z_T = 50$  a.u. The ionization cross sections are calculated with 20 impact parameters, which range from  $0 \rightarrow 14.0$  a.u. The trajectory effect can be studied by comparison of the cross sections calculated with CT and ST. Before we present our calculated ionization cross sections, we will first discuss the numerical accuracy and numerical convergence in the present calculations.

There have been many time-dependent Schrödinger equation studies of this simple collision system, but no two calculations are in good agreement within 10% over the whole energy region, especially on the lower-energy side (below 1 keV). In the present method, since we propagate the time-dependent wave function in the energy representation, we

TABLE I. Eigenenergies (a.u.) of H atoms calculated by the pseudospectral method.

	Exact	$\Delta E_{l=0}$	$\Delta E_{l=1}$	$\Delta E_{l=3}$	$\Delta E_{l=5}$
$n=1$	-5.0000E-01	-5.7E-15			
$n=3$	-5.5556E-02	4.3E-16	2.8E-16		
$n=5$	-2.0000E-02	-2.4E-16	5.5E-16	0.0E-00	
$n=7$	-1.0204E-02	6.6E-11	5.4E-11	1.8E-11	1.7E-12
$n=9$	-6.1728E-03	1.6E-05	1.4E-05	8.4E-06	2.8E-06

will first check the eigenenergies of H atoms in the pseudospectral grid. The calculated eigenenergies from Eq. (11) are very accurate for the lower excited states, as listed in Table I. Note that to show our numerical accuracy, we present the exact eigenenergies as well as the differences between the calculated eigenenergies and the exact ones. The calculated eigenenergies for the lower excited states ( $n < 7$ ) almost reach machine precision, and the numerical error increases as the principal quantum number  $n$  increases, as shown in Table I. For a given  $n$ , the numerical error decreases for the higher partial waves due to oscillating less. Overall, this pseudospectral grid can well describe the eigenwave-function of H atoms. With the pseudospectral grid, we perform a convergence check for a lower energy ( $E = 0.1$  keV) collision, which is the most difficult case in the present calculations, with different calculation parameters. To check the numerical convergence against the number of partial waves, we performed calculations with 10, 15, and 20 partial waves. The numerical results are already converged at ten partial waves. In a similar way, we also checked the convergence against the number of grid points. Three calculations were performed with 100, 150, and 200 radial grid points. Less than 2% error appear between points 100 and 150. The two results of 150 and 200 radial grid points agree with each other within less than 1%. All the final data presented in this work are calculated with 15 partial waves and 150 radial grid points. We also checked the convergence against the number of time steps by calculating the ionization probabilities with 2000, 4000, and 6000 time steps, as shown in Fig. 1. Two set calculations are presented in Fig. 1. One is a curved trajectory from Eq. (3), and the other is a straight-line trajectory calculation. The differences between the two calculations represent the trajectory effect. Since the antiproton and proton attract each other, the CT calculated ionization probabilities are larger than the ST calculated results. The calculated ionization probabilities with 2000 time steps are larger than the converged one (with 6000 time steps). In the time-dependent calculation, to avoid the electron wave-packet reflection when the electron reaches the boundary [26], we add a filter starting from  $r_w = 150$  a.u. The filter function  $W(r)$  used in the present calculation is

$$W(r) = \begin{cases} 1.0, & r \leq r_w \\ \cos^{1/4} \left( \frac{r - r_w}{r_{max} - r_w} \frac{\pi}{2} \right), & r > r_w. \end{cases} \quad (17)$$

After each time step, we multiply the wave function by the filter  $W(r)$ . This filter (or absorber) may induce an artificial

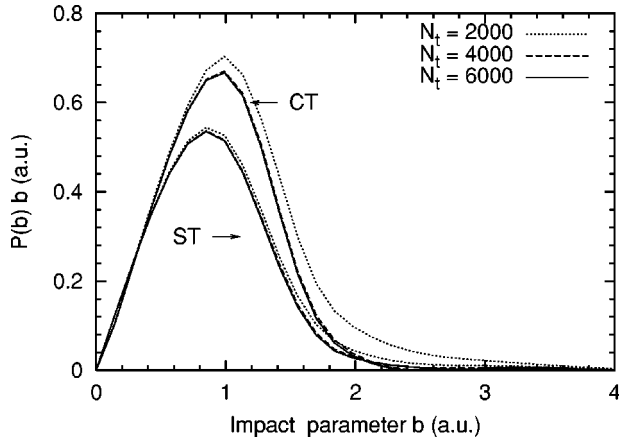


FIG. 1. The ionization probabilities calculated with 2000 (dotted curve), 4000 (dashed curve), and 6000 (solid curve) time steps in  $H + \bar{p}$  collisions at 0.1-keV collision energy. ST stands for the straight-line trajectory calculation, and CT stands for the curved trajectory calculation.

absorption. To check the validity of the filter, we see that ionization probabilities with a greater level of absorption (6000 time steps) do not increase as compared with those with a lower level of absorption (2000 time steps). This infers that the filter does not influence the final calculations.

In principle, we need to abstract the ionization probabilities when the antiproton is infinitely far from the target H atom. In practice, we abstract this ionization probability when the two particles separate from each other at some distance. Figure 2 shows dynamic ionization probabilities with different impact energies. Clearly, we see that the ionization probabilities saturate at 10 a.u. for the high-impact energy ( $E > 1$  keV). The ionization probability shows a rapid increase from  $-5.0$  to  $10$  a.u., followed by a slow increase for the low impact energy (0.1 keV). Thus, we should be careful to take a sufficiently long time until the probability become completely stable. This time delay can be understood as a post-collision interaction, as indicated by Pons [12]; i.e., due to the slow antiproton motion ( $v \sim 0.06$  a.u.),

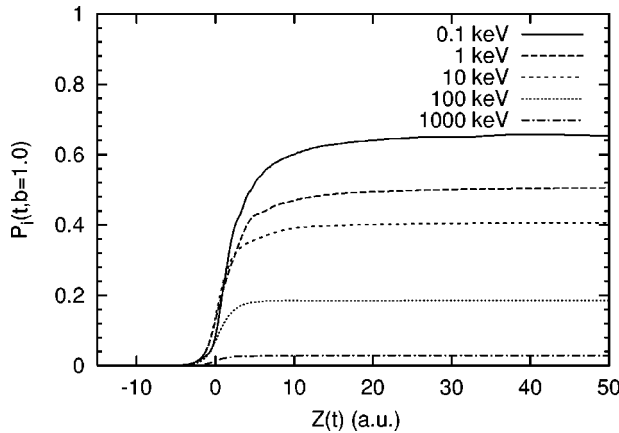


FIG. 2. The dynamic ionization probabilities in  $H + \bar{p}$  collisions at several impact energies with the impact parameter  $b = 1.0$ . The calculations are based on a curved trajectory.

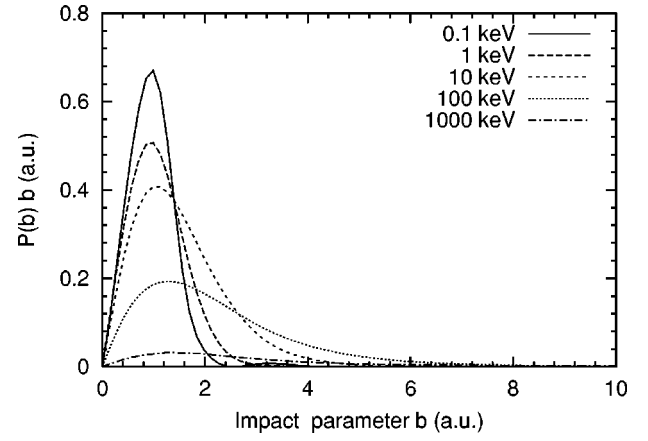


FIG. 3. The ionization probabilities in  $H + \bar{p}$  collisions as a function of impact parameter  $b$  at several impact energies.

an ejected electron is pushed out by the projectile even when the projectile is leaving the target H atom. After all these convergence checks, we will present our calculations.

#### IV. RESULTS AND DISCUSSION

Figure 3 shows ionization probabilities as functions of impact parameter  $b$  with different incident energies. Table II lists the impact parameter value  $b_{max}$ , corresponding to the maxima of  $bP(b)$ , and impact parameter value  $b_{1/2}$ , corresponding to the large position at which  $bP(b)$  is half of the peak value. When the incident energy is less than 25 keV in a laboratory frame (corresponding to a relative velocity  $v = 1.0$  a.u.),  $b_{max}$  is given by the radius of the hydrogen  $1s$  orbital. If the incident energy is above 25 keV,  $b_{max}$  is determined by the dynamic relationship between colliding particles. The relation between the most possible energy gain of an ejected electron and  $b_{max}$  can be predicted by Massey's criterion [27]:

$$\omega = v/b_{max}. \quad (18)$$

In the cases of impact energies 100 and 1000 keV, the most possible energy gains (ionization potential plus ejected electron's energy) are 1.6 and 4.2 a.u. If we replace  $b_{max}$  with  $b_{1/2}$  in Eq. (18), we can estimate the broadening of the ejected electron energy spectra, which are about 0.69 and 1.78 a.u. for 100 and 1000 keV. This means that the ejected electron energy spectrum moves to a higher energy, and is broadened for high-impact energy collisions.

TABLE II. Impact energy dependence of  $b_{max}$ ,  $b_{1/2}$ , and the mean excitation energy  $\omega$  obtained from Massey's criterion.

$E$ (KeV)	$v$ (a.u.)	$b_{max}$	$b_{1/2}$	$\omega$ (in a.u.)
0.1	0.0632	$\sim 1$	1.6	
1	0.2	$\sim 1$	1.8	
10	0.632	$\sim 1.1$	2.4	
100	2	1.2	2.8	1.6
1000	20	1.4	3.3	4.2



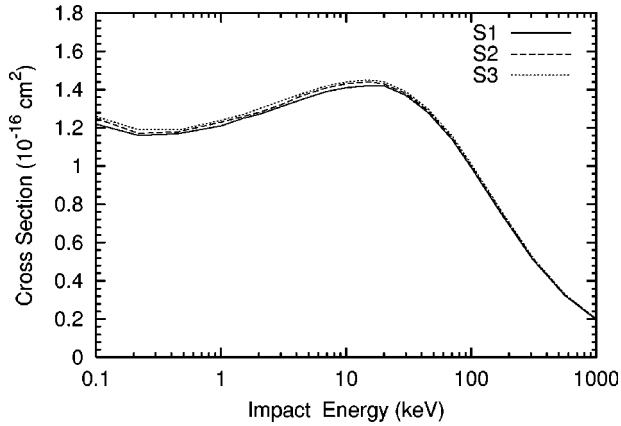


FIG. 4. The ionization cross sections of a H atom by antiproton impact calculated with three schemes  $S1$ ,  $S2$ , and  $S3$ . The definition of the three schemes is discussed in the text.

Normally, we calculate the ionization probability by subtracting all the bound-state probabilities from one, as

$$P^{ion}(T,b) = 1 - \sum_i |\langle \psi(T) | \psi_i \rangle|^2, \quad (19)$$

where  $\{\psi_i\}$  are all the bound states for the target H atom. This is because, in our calculations, the highly excited states ( $n > 10$ ) are not well described, as shown in Table I. To estimate the numerical uncertainty due to the highly excited states, we present the ionization cross section in the following three schemes.  $S1$ : we subtract all states with negative energies.  $S2$ : we subtract all the states with a calculated negative eigenenergy in agreement with the exact one within 5% error.  $S3$ : we subtract all states with a principal quantum number  $n \leq 10$ . The calculated ionization cross section with the three schemes are shown in Fig. 4. Since, in our calculations, all the states with a principal quantum number  $n \leq 10$  are described accurately, the  $S3$  curve gives the upper limit of the ionization cross section. Roughly speaking, the  $S1$  curve gives the lower limit of the ionization cross sections. The differences between the  $S1$  and  $S3$  curves represent the numerical uncertainty. The  $S2$  curve is between the two limits. Since the  $S1$  and  $S3$  curves are in good agreement with each other for high-energy calculations ( $E > 40$  keV), we can ignore the uncertainty due to the calculation scheme. In the lower-energy region, the differences between the  $S1$  and  $S2$  calculations are less than 3%. Therefore, we conclude that the numerical uncertainty of the ionization cross section is less than 3%.

Finally, we will present our calculated ionization cross sections based on the  $S1$  scheme with the CT trajectory (solid curves) and the ST trajectory (dashed curves) in Fig. 5. We present a comparison with other calculations [8,10,12,15,11] in Fig. 5(a), and a comparison with the experimental data [16] in Fig. 5(b). Above 1 keV, the discrepancy of the cross sections between the CT and ST calculations is less than 4%, but at 0.1 keV the discrepancy increases up to 20%. The CT cross section is larger than the ST cross section due to the proton-antiproton Coulombic at-

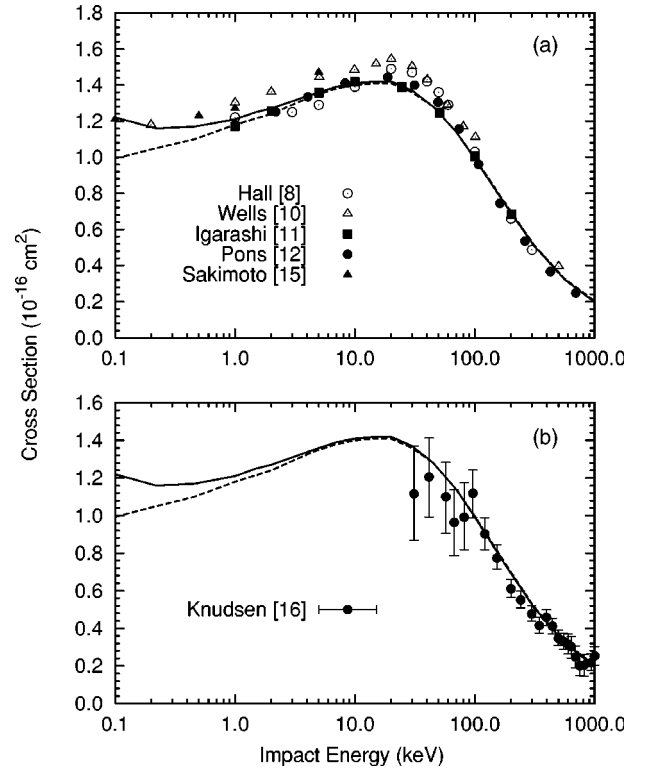


FIG. 5. Calculated ionization cross sections of H atom by antiproton impact in a wide energy range with a curved trajectory (solid curve) and a straight line trajectory (dashed curve). (a) Comparison with other calculations. (b) Comparison with the experiment.

traction. Here we clearly show that the trajectory effect plays an important role in the lower-energy collision. The simple straight-line trajectory calculation cannot give the right results within a 10% error in the lower-energy region.

The results of Ref. [10] are always larger than our results by 10%, except at 2 and 500 keV. The results of Ref. [8] are also larger than our results in the energy region from 10 to 150 keV, but smaller than our result when the impact energy is below 10 keV or above 150 keV. The results of Ref. [15] are always larger than our results by 10% except at 0.1 keV, at which the two agree with each other. Two other recent calculations [12,11] are closer to our calculations. Among the CC methods, Hall *et al.* [8] expanded the electronic wave function in terms of a finite Hilbert space set, Igarashi *et al.* [11] expanded the wave function by the Strumian basis set (associated Largurre basis set), and Pons [12] used the spherical Bessel functions to describe the continuum function. As for the direct solution methods, Wells *et al.* [10] used a numerical solution in three-dimensional Cartesian coordinate grids, and the ionization cross section was estimated using Eq. (19) with  $n=4$ .

Our calculated results are in good agreement with the experimental measurement [16] as shown in Fig. 5(b) over the whole experimental energy range. We hope new experimental data in the lower-energy region will be available soon.

To summarize, we have presented a theoretical study of the ionization process in  $H + \bar{p}$  collisions by solving the

time-dependent Schrödinger equation with the split-operator method and the generalized pseudospectral method in the energy representation. Particular attention was paid to the numerical accuracy and the numerical convergence. Our calculated results are confirmed to be accurate and stable, and consistent with various checks within a 3% discrepancy. The results are in reasonable agreement with the experimental

data. Since our time-dependent pseudospectral method can be used to describe very highly excited states as well as ground states [28], a combination of our time-dependent method with the time-dependent fully quantum-mechanical method used in the electron-impact ionization calculation studies [29] can be used to study the formation of protoniums.

- 
- [1] D. R. Bates and G. Griffing, Proc. Phys. Soc., London, Sect. A **66**, 961 (1953).
- [2] M. H. Martir, A. L. Ford, J. F. Reading, and R. L. Becker, J. Phys. B **15**, 1729 (1982).
- [3] J. Cohen, Phys. Rev. A **36**, 2074 (1987).
- [4] D. R. Schultz, Phys. Rev. A **40**, 2330 (1989).
- [5] P. D. Fainstein, V. H. Ponce, and R. D. Rivarola, J. Phys. B **24**, 3091 (1991).
- [6] N. Toshima, Phys. Lett. A **175**, 2024 (1993).
- [7] D. R. Schultz, P. S. K. Krstic, C. O. Reinhold, and J. C. Wells, Phys. Rev. Lett. **76**, 2882 (1996).
- [8] K. A. Hall, J. F. Reading, and A. L. Ford, J. Phys. B **29**, 6123 (1996).
- [9] P. S. Krstic, D. R. Schultz, and R. K. Janev, J. Phys. B **29**, 1941 (1996).
- [10] J. C. Wells, D. R. Schultz, P. Gavras, and M. S. Pindzola, Phys. Rev. A **54**, 593 (1996).
- [11] A. Igarashi, S. Nakazaki, and A. Ohsaki, Phys. Rev. A **61**, 062712 (2000).
- [12] B. Pons, Phys. Rev. Lett. **84**, 4569 (2000).
- [13] B. Pons, Phys. Rev. A **63**, 012704 (2001).
- [14] K. Sakimoto, J. Phys. B **33**, 3149 (2000).
- [15] K. Sakimoto, J. Phys. B **33**, 5165 (2000).
- [16] H. Knudsen *et al.*, Phys. Rev. Lett. **74**, 4627 (1995).
- [17] ASACUSA Collaboration, CERN Report No. CERN/SPC, p. 307 (unpublished).
- [18] X. M. Tong, D. Kato, T. Watanabe, and S. Ohtani, Phys. Rev. A **62**, 052701 (2000).
- [19] X. M. Tong, D. Kato, T. Watanabe, and S. Ohtani, J. Phys. B **33**, 5585 (2000).
- [20] J. Cohen, Phys. Rev. A **56**, 3583 (1997).
- [21] V. I. Korobov and I. Shimamura, Phys. Rev. A **56**, 4587 (1997).
- [22] X. M. Tong and S. I. Chu, Chem. Phys. **217**, 119 (1997).
- [23] G. Yao and S. I. Chu, Chem. Phys. Lett. **204**, 381 (1993).
- [24] M. R. Hermann and J. A. Fleck, Jr., Phys. Rev. A **38**, 6000 (1988).
- [25] T. F. Jiang and S. I. Chu, Phys. Rev. A **46**, 7322 (1992).
- [26] E. Y. Sidky and E. D. Esry, Phys. Rev. Lett. **85**, 5086 (2000).
- [27] N. F. Mott and E. C. Bullard, in *The Theory of Atomic Collisions*, 3rd ed. (Oxford University Press, London, 1965), Chap. XIX, p. 665.
- [28] X. M. Tong and S. I. Chu, Phys. Rev. A **61**, 031401R (2000).
- [29] D. O. Odero, J. L. Peacher, D. R. Schultz, and D. H. Madison, Phys. Rev. A **63**, 022708 (2001).